Talanta 119 (2014) 341–347

Contents lists available at ScienceDirect

Talanta

journal homepage: www.elsevier.com/locate/talanta

Fe_3O_4@ionic liquid@methyl orange nanoparticles as a novel nano-adsorbent for magnetic solid-phase extraction of polycyclic aromatic hydrocarbons in environmental water samples

Xiaofei Liu [a], Xin Lu [a,*], Yong Huang [a], Chengwei Liu [b], Shulin Zhao [a,**]

[a] College of Chemistry and Pharmacy, Guangxi Normal University, Guilin 541004, China
[b] Department of Anatomy, Guilin Medical College, Guilin 541004, China

ARTICLE INFO

Article history:
Received 28 August 2013
Received in revised form
9 November 2013
Accepted 13 November 2013
Available online 20 November 2013

Keywords:
Fe_3O_4@ionic liquid@methyl orange nanoparticles
Self-assembly
Magnetic solid-phase extraction
Polycyclic aromatic hydrocarbons
Environmental water samples

ABSTRACT

A novel nano-adsorbent, Fe_3O_4@ionic liquid@methyl orange nanoparticles (Fe_3O_4@IL@MO NPs), was prepared for magnetic solid-phase extraction (MSPE) of polycyclic aromatic hydrocarbons (PAHs) in environmental water samples. The Fe_3O_4@IL@MO NPs were synthesized by self-assembly of the ionic liquid 1-octadecyl-3-methylimidazolium bromide (C18mimBr) and methyl orange (MO) onto the surface of Fe_3O_4 silica magnetic nanoparticles, as confirmed by infrared spectroscopy, ultraviolet–visible spectroscopy and superconducting quantum interface device magnetometer. The extraction performance of Fe_3O_4@IL@MO NPs as a nano-adsorbent was evaluated by using five PAHs, fluorene (FLu), anthracene (AnT), pyrene (Pyr), benzo(a)anthracene (BaA) and benzo(a)pyrene (BaP) as model analytes. Under the optimum conditions, detection limits in the range of 0.1–2 ng/L were obtained by high performance liquid chromatography–fluorescence detection (HPLC–FLD). This method has been successfully applied for the determination of PAHs in environmental water samples by using the MSPE–HPLC–FLD. The recoveries for the five PAHs tested in spiked real water samples were in the range of 80.4–104.0% with relative standard deviations ranging from 2.3 to 4.9%.

1. Introduction

Solid phase extraction (SPE) is one of the most commonly used pre-treatment and pre-concentration techniques for the analysis of pollutants in environmental and biological samples. However, traditional SPE techniques require passing samples completely through cartridges filled with sorbents, followed by eluting the analytes with organic solvents. This method is tedious, time-consuming, relatively expensive and labor intensive, especially for large volumes of samples. To address these limitations, a new SPE technique called magnetic solid-phase extraction (MSPE), based on the use of magnetic or magnetically modified adsorbents, was developed and applied to bioseparation and chemical analysis [1–4]. In MSPE procedures, the magnetic adsorbents are exposed in the sample solution to adsorb the analytes and then collect the analytes by an external magnetic field, which greatly simplifies the SPE procedure [5,6] and enhances extraction efficiency. Thus, some efforts have been made in recent years to develop various magnetic nano-adsorbents, and further exploit their potential applications in MSPE [7–15]. For example, Cai's group reported the use of mixed hemimicelle and octadecyl (C18) functionalised magnetic nanocomposites (MNPs) as sorbents for the extraction of target compounds [16–18]. Wang et al. evaluated graphene-based MNPs for the MSPE of carbamate pesticides from environmental water samples [19]. Pardasani et al. used multi-walled carbon nanotube functionalised MNPs as sorbents for dispersive solid phase extraction of nerve agents and their markers from muddy water [20]. Although substantial progress has been made, new magnetic adsorbents with simple preparation processes, low price and high adsorption efficiencies are still highly desirable.

Ionic liquids (ILs) are a class of organic salts that possess unique chemical and physical properties, such as good stability, tuneable miscibility with water, high conductivity, and high heat capacity [21,22]. These attractive properties make them promising materials for a number of analytical applications [23–25]. Specifically, ILs have been widely used for sample pre-treatment, including liquid–liquid extraction [26,27], liquid-phase microextraction [28,29], and solid-phase microextraction [30,31]. For example, Pino's group applied the ionic liquid 1-hexadecyl-3-methylimidazolium bromide in a microwave-assisted liquid–liquid extraction system for polycyclic aromatic hydrocarbons (PAHs) in sediments [32]. Yao et al. have investigated ionic liquid-coated Fe_3O_4 MNPs as an adsorbent of mixed hemimicelles solid-phase extraction for the

* Corresponding author. Tel.: +86 773 5846279; fax: +86 773 2120958.
** Corresponding author. Tel.: +86 773 5856104; fax: +86 773 5832294.
E-mail addresses: luxin-chem@163.com (X. Lu), zhaoshulin001@163.com (S. Zhao).

0039-9140/$ - see front matter
http://dx.doi.org/10.1016/j.talanta.2013.11.039

pre-concentration of PAHs from environmental samples [33]. However, exploration of ILs in SPE is still at an early stage.

In the present work, we have prepared a novel nano-adsorbent, Fe_3O_4@ionic liquid@methyl orange nanoparticles (Fe_3O_4@IL@MO NPs) through self-assembly. This new type of nano-adsorbent combines the advantages of the IL, MO and the MNPs. Compared with the previously reported works [34,35], this nano-adsorbent based MSPE provides a facile, rapid, and efficient sample preparation process, which enables the treatment of large volume samples in a short period of time. To the best of our knowledge, this is the first example of the Fe_3O_4@IL@MO nano-adsorbent for MSPE. Five PAHs, including fluorene (FLu), anthracene (AnT), pyrene (Pyr), benzo(a)anthracene (BaA) and benzo(a)pyrene (BaP), were selected as model analytes to evaluate the extraction performance of the prepared nano-adsorbent. Various experimental parameters that could affect the extraction efficiencies were also investigated. The results revealed that the prepared nano-adsorbent exhibited excellent adsorption properties. Furthermore, the application of such Fe_3O_4@IL@MO nano-adsorbent for the determination of the PAHs in environmental water samples using high performance liquid chromatography–fluorescence detection (HPLC–FLD) was also demonstrated.

2. Experimental

2.1. Chemicals and materials

FLu, AnT, Pyr, BaA and BaP were purchased from Aladdin (Guangzhou, China). The C18mimBr IL was purchased from Lanzhou Greenchem ILs, LICP, CAS (Lanzhou, China). Magnetic Fe_3O_4/SiO_2 NPs with particle size of 100 nm were purchased from Chemicell GmbH (Berlin, Germany). Methyl orange (MO) was purchased from Shanghai Reagent Factory (Shanghai, China). HPLC grade methanol and acetonitrile were obtained from J&K Chemical (Beijing, China). Sodium hydroxide (NaOH) was purchased from Sinopharm Chemical Reagent (Shanghai, China). All other reagents were of analytical grade. Water was purified by employing a Milli-Q plus from Millipore (Bedford, MA, USA) and used throughout this work.

The standard stock solutions of FLu, AnT, Pyr, BaA and BaP (1 mg/mL) were prepared in methanol, and the work solutions were freshly prepared by diluting the stock solution with mobile phase before used. The stock solution of C18mimBr (20 mg/mL) was prepared in methanol and water (v:v=50:50), and the working solutions were prepared daily by diluting the stock solution with water to the required concentrations. The stock solution of MO (4 mg/mL) was prepared in water.

2.2. Synthesis of Fe_3O_4@IL@MO nano-adsorbent

The Fe_3O_4@IL@MO NPs were synthesized by the protocol shown in Scheme 1A. First, 500 μL of Fe_3O_4/SiO_2 NPs (12 mg/mL) and 500 μL of C18mimBr IL solution (15 mg/mL) were added to a 5-mL centrifuge tube. The mixture was sonicated for 15 min to ensure complete self-assembly of C18mimBr IL onto Fe_3O_4/SiO_2 NPs. Next, MO was added to the mixture and sonicated for another 25 min to promote MO self-assembly on the Fe_3O_4@IL NPs through electrostatic and hydrophobic interactions. Finally, a strong magnet was applied to the outside of the centrifuge tube, and the Fe_3O_4@IL@MO NPs were separated from the solution. After 5 min, the solution became limpid and the supernatant was decanted away.

2.3. Characterization

Infrared spectra of the nanoparticles were recorded with a Fourier transform infrared spectrometer (FT-IR, Perkin Elmer Inc) in the wavelength range of 4000–500 cm^{-1} with a resolution of 2 cm^{-1} by pressing a small amount of nanoparticles into a KBr pellet. The UV/vis spectra of isolated Fe_3O_4/SiO_2 NPs, Fe_3O_4@IL NPs and Fe_3O_4@IL@MO NPs were collected using a TU-1901 UV–vis spectrophotometer (Beijing Purkinje General Instrument Co., Ltd., China) with a resolution of 0.5 nm. Magnetization measurement was carried out with a superconducting quantum interface device (SQUID) magnetometer (Quantum Design MPMS XL) at 300 K.

2.4. Sample collection

All environmental water samples were obtained from different districts of Guilin. River water sample was acquired from Lijiang River (Guilin, China). Wastewater sample, containing 90% domestic wastewater and 10% industiral wastewater, was supplied by Wulidian Wastewater Treatment Plants (Guilin, China). All samples were collected randomly and filtered through 0.45 μm membranes to remove suspended particles before analysis.

2.5. MSPE procedure

The MSPE procedure is shown in Scheme 1B. First, Fe_3O_4@IL@MO NPs were added to a 150-mL water sample containing FLu, AnT, Pyr, BaA and BaP (pH 8.0), and the mixture was placed on a slow-moving platform shaker and allowed to equilibrate for 15 min at 35 °C. Then, a strong magnet was applied to the bottom of the beaker, isolating the Fe_3O_4@IL@MO NPs from the suspension. After 10 min, the suspension was decanted and the residual solution of Fe_3O_4@IL@MO NPs was transferred to a 2-mL centrifuge tube. The Fe_3O_4@IL@MO NPs were aggregated again by positioning a magnet to the outside of the tube wall so that the residual solution could be completely removed by pipette. Finally, the isolated nanoparticles were mixed with 1500 μL of acetonitrile (pH 9.0, containing 2% (v/v) 1 M NaOH) and sonicated for 1 min to elute the pre-concentrated target analytes. Afterwards, a magnet was positioned on the outside of the centrifuge tube, and the supernatant solution was collected using a micropipette. The supernatant solution was dried under a mild nitrogen stream. The residue was re-dissolved in 150 μL of acetonitrile, of which 20.0 μL was injected into the HPLC system for the detection of the target analytes.

2.6. HPLC analysis

An HPLC (Shimadzu, Japan) system was used for the determination of PAHs. The system consisted of a binary LC-10ATvp pump, an RF-10Avp FLD detector, a CTO-10ASvp column oven and an SCL-10Avp system controller. The analytical column was a 250 mm × 4.6 mm i.d. Diamonsil C18 (2) column (Dikma Technologies Inc., China), and the injection loop volume was 20 μL. The mobile phase consisted of acetonitrile as solvent A and water–methanol (70:30, v-v) as solvent B. The gradient elution program was started at 85% A during the first 5 min, increased to 100% A over 0.5 min and kept for 9.5 min, then decreased to 85% A over 1 min and kept for 5 min to equilibrate the column. The flow rate of the mobile phase was set at 1.0 mL/min. The time program of fluorescence detection was as follows: Flu (0–7.3 min, λ_{ex} 270 nm, λ_{em} 323 nm); AnT (7.3–8.3 min, λ_{ex} 252 nm, λ_{em} 402 nm); Pyr (8.3–10 min, λ_{ex} 270 nm, λ_{em} 390 nm); BaA (10–12 min, λ_{ex} 270 nm, λ_{em} 390 nm) and BaP (12–20 min, λ_{ex} 290 nm, λ_{em} 410 nm). The column oven temperature was maintained at 25 °C.

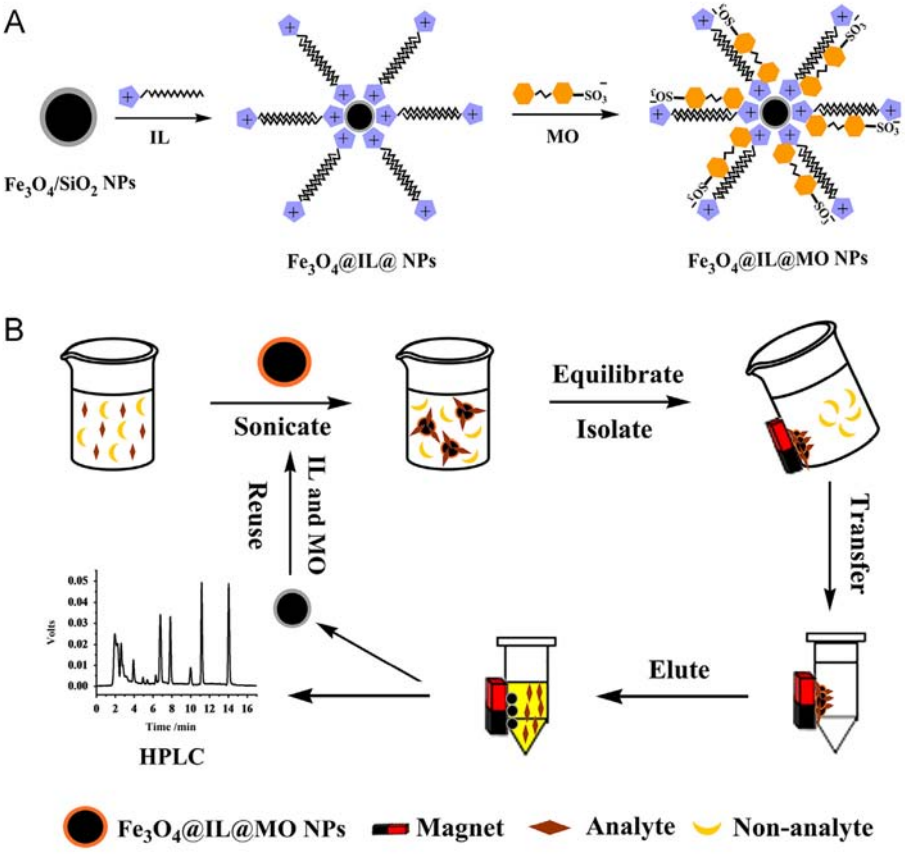

Scheme 1. (A) The self-assembly procedure for Fe_3O_4@IL@MO NPs, and (B) procedure for MSPE of the target PAHs using Fe_3O_4@IL@MO NPs.

3. Results and discussion

3.1. Characterization of Fe_3O_4@IL@MO nano-adsorbent

The UV/vis measurements were first carried out to investigate the assembly of ILs and MO onto Fe_3O_4/SiO_2 NPs, the results of which are shown in Fig. S1. Without ILs and MO, the UV/vis spectrum of Fe_3O_4/SiO_2 NPs did not show an absorption peak between 300 nm and 600 nm (curve a). After incubation of the ILs with Fe_3O_4/SiO_2 NPs, an absorption peak at 466 nm was observed, indicating the successful assembly of ILs at the surface of Fe_3O_4/SiO_2 NPs (curve b). Curve c depicts the UV/vis spectrum of Fe_3O_4@IL NPs after assembly with MO. Compared with curve b, a new absorption peak at 426 nm from MO was observed. This result demonstrated that MO had been assembled onto the surface of Fe_3O_4@IL NPs.

The assembly of ILs and MO onto Fe_3O_4/SiO_2 NPs was further confirmed by FT-IR measurements. Fig. 1 depicts the FT-IR spectra of Fe_3O_4/SiO_2 NPs before and after self-assembly with ILs and MO. Before assembly, the Fe_3O_4/SiO_2 NPs only showed the signal of Si–O–Si at 1092 cm^{-1}. After assembly with ILs, the signals at 2923 and 2852 cm^{-1} were attributed to C–H stretches within the octadecyl chain. Furthermore, the signals near 1637 and 1467 cm^{-1} were attributed to the characteristic signals of imidazolium in Fe_3O_4@IL NPs [35]. In the case of Fe_3O_4@IL@MO NPs, additional characteristic signals were evident at 1611 cm^{-1} for the phenyl bond stretching vibration and at 1372, 1216 and 1120 cm^{-1} for the sulfonic asymmetric stretching [35,36], demonstrating the successful assembly of ILs and MO on the surface of Fe_3O_4/SiO_2 NPs.

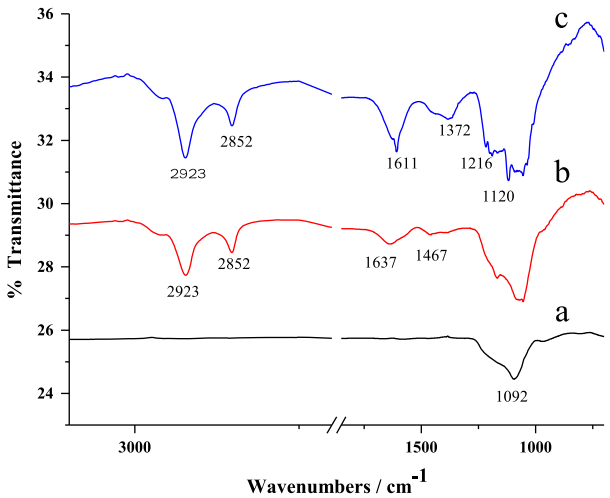

Fig. 1. FT-IR spectra of (a) Fe_3O_4/SiO_2 NPs, (b) Fe_3O_4@IL NPs, and (c) Fe_3O_4@IL@MO NPs.

In addition, magnetic properties of Fe_3O_4/SiO_2 NPs before and after self-assembly with ILs and MO were also investigated, and the results are shown in Fig. 2. Both Fe_3O_4/SiO_2 NPs and Fe_3O_4@IL@MO NPs exhibited typical superparamagnetic behavior due to no hysteresis, remanence and coercivity. The maximal saturation magnetizations of Fe_3O_4/SiO_2 NPs and Fe_3O_4@IL@MO NPs were 57.86 and 48.02 emu/g, respectively. The decrease of maximal saturation magnetizations of Fe_3O_4@IL@MO NPs resulted from the nonmagnetic IL and MO shell. It had been reported that

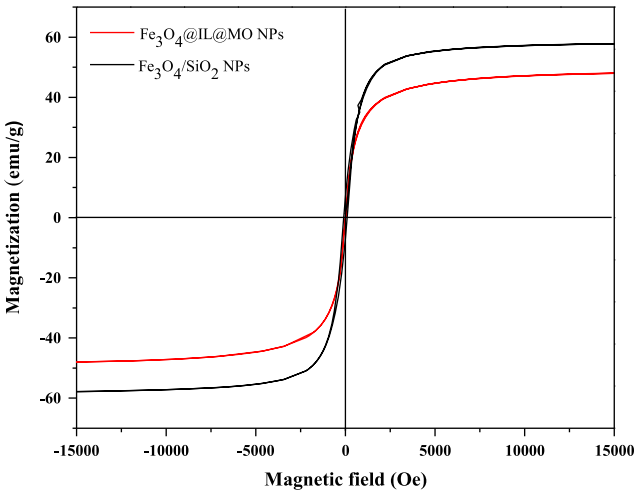

Fig. 2. Magnetic hysteresis loops of the Fe_3O_4/SiO_2 NPs and Fe_3O_4@IL@MO NPs.

the saturation magnetization of 16.3 emu/g was sufficient for magnetic separation with a magnet [37]. Thus, the Fe_3O_4@IL@MO NPs prepared here could be readily separated from solution with a magnet due to their superparamagnetism and large saturation magnetization.

3.2. Optimization of the extraction process

To improve the extraction efficiency of MSPE for the extraction of the PAHs using Fe_3O_4@IL@MO nano-adsorbent, the relevant experimental parameters, such as the amount of Fe_3O_4@IL@MO NPs, pH value, extraction time, extraction temperature, eluent type and volume, elution time, and sample volume were examined. In these experiments, the chromatographic peak area from assaying a mixed sample solution containing 80 ng/L FLu, 80 ng/L AnT, 150 ng/L Pyr, 150 ng/L BaA and 80 ng/L BaP, was recorded. Experimental conditions were optimized based on the averaged results from three assays when the relative standard deviation (RSD) of each test point was less than 5.0%.

3.2.1. Effect of the amount of nano-adsorbent

The amount of nano-adsorbent (Fe_3O_4@IL@MO NPs) has a significant influence on the extraction efficiency of PAHs. To improve the extraction efficiency, different amounts of Fe_3O_4@IL@MO NPs were tested in the range of 5–22 mg, and the results are shown in Fig. 3. The extraction efficiency increases gradually with increasing amounts of Fe_3O_4@IL@MO NPs. The maximum extraction efficiency was obtained when the amount of Fe_3O_4@IL@MO NPs was 18 mg. According to the above results, 18 mg was selected as the optimal amount of Fe_3O_4@IL@MO NPs for MSPE.

3.2.2. Effect of pH value

The pH value is a crucial factor in the extraction process because it not only affects the existing form of the MO [38], but also can change the density of the negative charge on the surface of Fe_3O_4@IL@MO NPs. Thus, it was necessary to investigate the effect of pH value on the extraction efficiency. As shown in Fig. 4, the extraction efficiency increased when increasing the pH value from 5.0 to 8.0. Further increasing the pH value, the extraction efficiency of FLu and AnT further increased, and reach the maximum at pH 10.0. At the same time, the extraction efficiency of Pyr, BaA and BaP decreased gradually. By weighing the extraction efficiency for all analytes, pH 8.0 was selected for the subsequent assays.

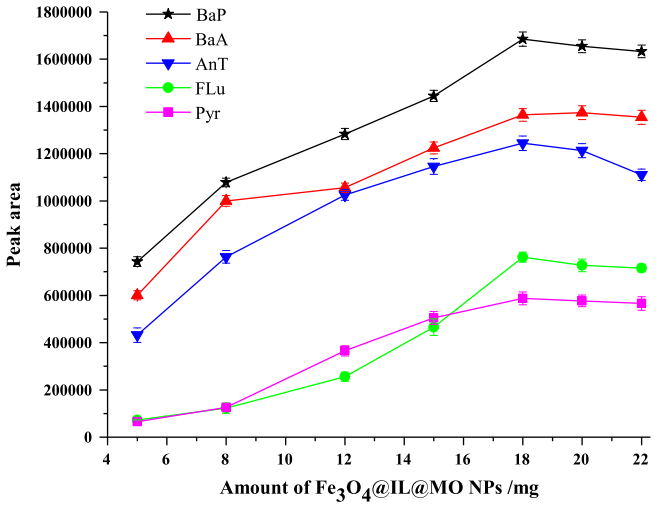

Fig. 3. Effect of the amount of Fe_3O_4@IL@MO NPs on the adsorption of the five PAHs. Extraction conditions: sample solution, 150 mL containing 80 ng/L Flu, 80 ng/L AnT, 150 ng/L Pyr, 150 ng/L BaA and 80 ng/L BaP; solution pH, 8.0; extraction time, 15 min; extraction temperature, 35 °C; and 1500 μL of acetonitrile containing 2% (v/v) 1 M NaOH (pH 9.0) as eluent.

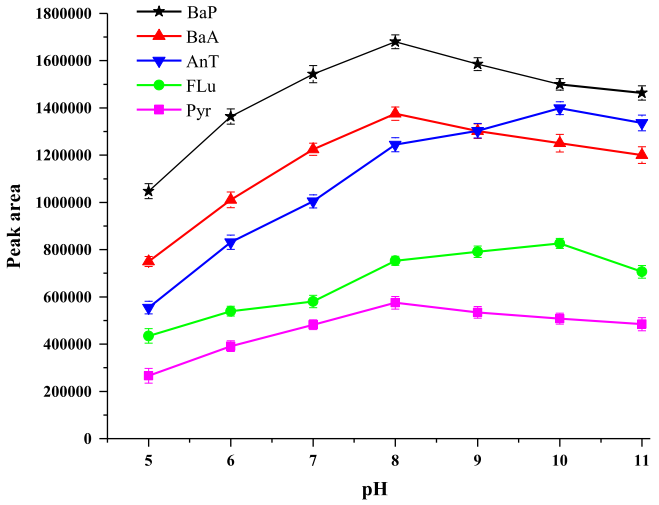

Fig. 4. Effect of solution pH on the adsorption of the five PAHs. The amount of Fe_3O_4@IL@MO NPs was 18 mg. Other extraction conditions are as indicated in Fig. 3.

3.2.3. Effect of extraction temperature

The temperature also affects the efficiency of extraction. High temperatures could reduce the distribution coefficient of the analyte and increase its diffusion coefficient, which is conducive to the rapid transition of the analyte to the solid phase extraction sorbent. Alternatively, the adsorption process can be exothermic so that when the temperature rises to a certain temperature, the analytes may be desorbed from the nano-adsorbent. To achieve better extraction efficiency, the effect of the extraction temperature was studied by varying the temperature from 25 °C to 60 °C. As shown in Fig. S2, the maximum extraction efficiency was obtained for Pyr, BaA and BaP when 35 °C was used. However, the maximum extraction efficiency for FLu and AnT was obtained at 40 °C and 50 °C, respectively. By considering the extraction efficiency for all five PAHs tested, 35 °C was selected for MSPE.

3.2.4. Effect of extraction time

To evaluate the effect of extraction time on the extraction efficiency of the PAHs, extraction times ranging from 5 to 25 min were tested, the results of which are shown in Fig. S3. As the

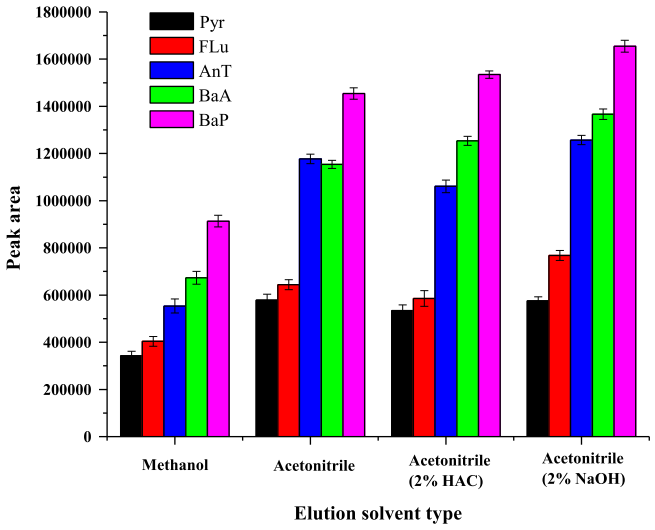

Fig. 5. Effect of elution solvent type on the adsorption of the five PAHs. The amount of Fe_3O_4@IL@MO NPs was 18 mg, and the pH value of sample solution is 8.0. Other extraction conditions are as indicated in Fig. 3.

extraction time increased, the extraction efficiency gradually increased and then remained nearly constant after 15 min. Thus, 15 min was selected as the optimal extraction time.

3.2.5. *Effect of elution conditions*

Desorption of the analytes from the magnetic nano-adsorbents was studied using different organic eluent solutions, including methanol and acetonitrile. The results are shown in Fig. 5. As seen, the eluting power of acetonitrile containing 2% (v/v) 1 M NaOH (pH 9.0) was much stronger than the methanol eluent solutions. Thus, acetonitrile at pH 9.0 was selected as the desorption solvent. Additionally, the effect of eluent solution volume on desorption efficiency of the analytes was also investigated. It was found that all the analytes could be quantitatively desorbed from the sorbent by rinsing the nano-adsorbent with 1500 μL of acetonitrile at pH 9.0. Therefore, 1500 μL of acetonitrile at pH 9.0 was selected for elution of the analytes from the nano-adsorbent.

3.2.6. *Effect of sample volume*

To achieve better extraction efficiency and higher preconcentration factor with shorter operational time, the effect of the sample volume was studied by using a series of different volume of sample solutions (50–300 mL) with the fixed amount of all analytes and the nano-adsorbent. As shown in Fig. S4, for solution volume more than 150 mL, the insufficient recovery were obtained. Thus, 150 mL was considered to be the optimal sample volume.

3.2.7. *Reusability of the Fe_3O_4/SiO_2 NPs*

In order to investigate the recycling of the Fe_3O_4/SiO_2 NPs, they were washed with 2 mL acetonitrile for twice after each MSPE run, and subsequently assembled with IL and MO. Each re-prepared nano-adsorbent was used for MSPE. The experimental results are shown in Fig. S5. It was clear that no obvious loss of the sorption capacity occurred after ten times of recycling. These results indicated that the self-assembly does not influence the stability of the Fe_3O_4/SiO_2 NPs for reusability.

3.3. *Analytical performance*

The proposed method was evaluated by using the MSPE–HPLC–FLD in terms of the response linearity, limit of detection, and reproducibility. Calibration curves were prepared by assaying standard solutions containing five PAHs at concentrations ranging from 4 to 400 ng/L for FLu, 0.5 to 400 ng/L for AnT, 4 to 800 ng/L for Pyr, 4 to 800 ng/L for BaA and 2 to 800 ng/L for BaP. Detection limits for the five PAHs were estimated from the IUPAC method [39,40]. The results are shown in Table 1. As seen, linear calibration curves were obtained with correlation coefficients (R^2) ranging from 0.9984 to 0.9999. The limits of detection were in the range of 0.1–2 ng/L. The reproducibility was studied by separating a mixture containing FLu, AnT, Pyr, BaA and BaP at 80, 40, 80, 80 and 40 ng/L, respectively, five times. The results indicated that the RSDs ($n=5$) for all analytes were $\leq 3.7\%$. In addition, the selectivity of the Fe_3O_4@IL@MO NPs for MSPE–HPLC–FLD was also investigated by analyzing other targets such as bisphenol A, 4-tert-octylphenol, 4-n-nonylphenol, naphthylamine, benzidine, 2-chlorophenol, 2,4-dichlorophenol and 2,4,6-trichlorophenol. It was found that none of them was detected under the selected HPLC–FLD conditions (data not shown). These results indicated that the present MSPE–HPLC–FLD method for the detection of the PAHs had high selectivity.

Table 1
Concentration linear ranges and detection limits of the PAHs.

Analyte	Regression equation	Linear range (ng/L)	Correlation coefficient (R^2)	LOD (ng/L)	RSD (%, $n=5$)
FLu	$A=5260.9C+345631$	4–400	0.9984	1	3.0
AnT	$A=13901C+237650$	0.5–400	0.9992	0.1	2.8
Pyr	$A=3776.6+9067.6$	4–800	0.9995	2	3.7
BaA	$A=9991.2-34241$	4–800	0.9996	0.8	2.3
BaP	$A=18972C+86606$	2–800	0.9999	0.4	1.7

3.4. *Enrichment effect of the MSPE method*

To evaluate the enrichment effect, the detection of five PAHs tested in standard solutions was conducted by the HPLC–FLD before and after MSPE using the Fe_3O_4@IL@MO nano-adsorbent. The detection limits for the five PAHs between enrichment and non-enrichment were compared. The results are shown in Table S1 with detection limits of enrichment found in the range of 0.1–2 ng/L. The detection limits of non-enrichment were in the range of 100–750 ng/L. These results indicate that the sensitivity of the MSPE–HPLC–FLD method was improved by 150–1000 times, which arosed from the high extraction efficiency. According to the previously reported results [35], the high extraction efficiency was attributed to the fact that the PAHs can interact with the Fe_3O_4@IL@MO nano-adsorbents via the hydrophobic and π–π interactions between the PAHs and the functionalized groups (azobenzene and imidazolium) of the nano-adsorbents. The multiple interactions were also the mechanism of the extraction of the PAHs with the nano-adsorbents.

3.5. *Analysis of environmental water samples*

The proposed method was further applied to the analysis of PAHs in environmental water samples. Fig. 6A shows the typical HPLC chromatograms of the spiked river water samples before and after extraction. As shown in Fig. 6A, no peaks from the PAHs tested were observed in the chromatogram before extraction of PAHs from the spiked water sample (trace a). This observation indicated that HPLC could not directly detect FLu, AnT, Pyr, BaA and BaP at the spiked concentration. After extraction of PAHs from the spiked water sample using Fe_3O_4@IL nano-adsorbents, five small peaks from the PAHs tested were observed (Fig. 6A, trace b). This demonstrated that the Fe_3O_4@IL nano-adsorbent has weak

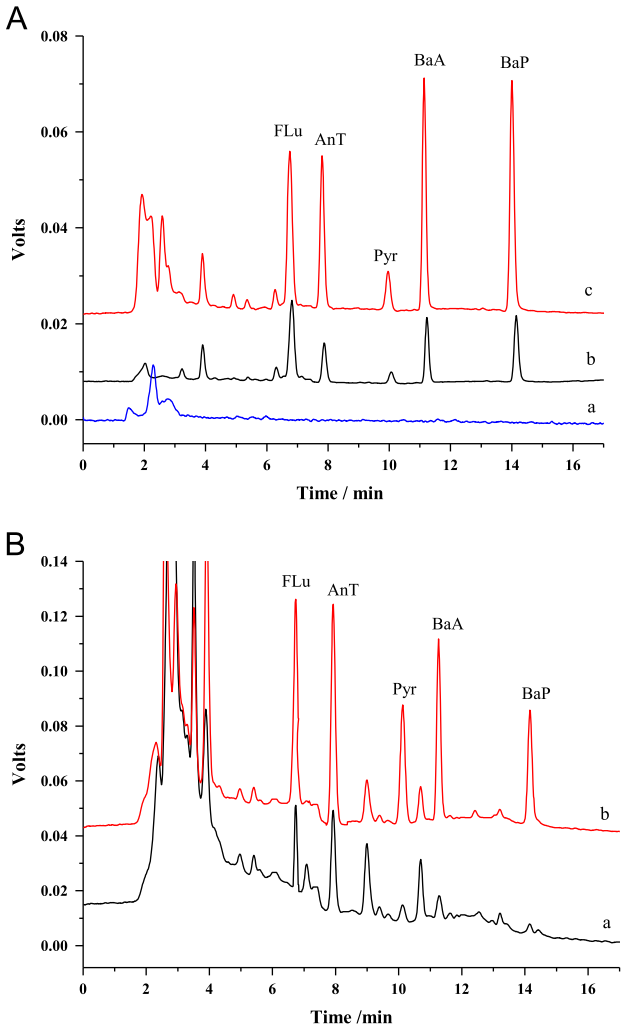

Fig. 6. (A) HPLC–FLD chromatograms of the river water sample spiked with 20 ng/L FLu, 10 ng/L AnT, 20 ng/L Pyr, 40 ng/L BaA and 20 ng/L BaP: (a) river water sample without MSPE, (b) river water sample after MSPE using Fe_3O_4@IL NPs, and (c) river water sample after MSPE using Fe_3O_4@IL@MO NPs. (B) HPLC–FLD chromatograms of the wastewater sample (a) and wastewater sample spiked with 80 ng/L FLu, 40 ng/L AnT, 100 ng/L Pyr, 40 ng/L BaA and 15 ng/L BaP (b).

extraction power to extract PAHs. However, when Fe_3O_4@IL@MO nano-adsorbents were used, five peaks from the PAHs tested were also observed, and the intensity of these peaks was much stronger than that obtained from Fe_3O_4@IL nano-adsorbents (Fig. 6A, trace c). This result demonstrated higher extraction efficiency of Fe_3O_4@IL@MO nano-adsorbents than Fe_3O_4@IL nano-adsorbents. The assay results of FLu, AnT, Pyr, BaA and BaP from the spiked water samples by HPLC–FLD using MSPE with Fe_3O_4@IL@MO nano-adsorbents are listed in Table 2. The recoveries for the five PAHs tested in spiked water samples were in the range from 81.6 to 104.0% with RSDs ($n=5$) ranging from 2.3 to 4.9%. Then, the MSPE–HPLC–FLD method was used for determination of PAHs in the wastewater sample. Fig. 6B shows the HPLC chromatograms of the wastewater sample and the wastewater sample after spiking standard PAHs. The results from the sample analysis are also summarized in Table 2. The recoveries of FLu, AnT, Pyr, BaA and BaP in wastewater sample analysis were found to be in the range of 80.4–100.4% with RSDs ($n=5$) ranging from 2.4 to 4.9%. These results indicated that the prepared Fe_3O_4@IL@MO nano-adsorbents could be used for extraction and analysis of PAHs in real water samples.

Table 2
Determination and recoveries of the PAHs in environmental water samples.

PAHs	Spiked (ng/L)	Lijiang water ($n=5$)			Spiked (ng/L)	Wastewater ($n=5$)		
		Found (ng/L)	Recovery (%)	RSD (%)		Found (ng/L)	Recovery (%)	RSD (%)
FLu	0	Not detected	–	–	0	5.87	–	–
	5	5.1	102.0	4.6	2	7.6	86.5	4.6
	80	75.5	94.4	3.7	6	10.8	82.2	4.9
	300	275.4	91.8	2.5	20	22.2	81.7	3.2
AnT	0	Not detected	–	–	0	8.46	–	–
	5	4.6	92.0	4.3	4	12.1	91.0	4.7
	80	81.2	101.5	2.3	10	18.2	97.4	2.8
	300	275.4	89.2	3.6	50	56.3	95.7	3.6
Pyr	0	Not detected	–	–	0	14.58	–	–
	10	10.4	104.0	4.9	5	18.6	80.4	3.2
	100	81.6	81.6	4.2	15	28.1	90.1	4.3
	600	520.2	86.7	3.9	60	71.2	94.4	3.8
BaA	0	Not detected	–	–	0	11.68	–	–
	10	10.1	101.0	4.4	5	16.7	100.4	4.2
	100	88.9	88.9	2.8	10	20.8	91.2	3.1
	600	523.8	87.3	3.5	50	55.5	87.6	2.4
BaP	0	Not detected	–	–	0	Not detected	–	–
	10	10.3	103.0	4.1	5	4.3	86.0	3.3
	100	96.6	96.6	3.6	10	9.06	90.6	4.9
	600	542.4	90.4	3.1	50	47.4	94.8	2.9

4. Conclusions

In summary, we have developed a novel nano-adsorbent, Fe_3O_4@IL@MO NPs, for MSPE of PAHs from environmental water samples. The magnetic nano-adsorbent is prepared by a self-assembly technique, which is very simple and mild. Compared with traditional SPE, this MSPE based on the Fe_3O_4@IL@MO NPs as an SPE adsorbent is fast, and the adsorbent can be easily separated from the sample solution. Moreover, this nano-adsorbent has a high extraction capacity and high enrichment factors and is able to treat large-volume samples in a short period of time. The benzene rings of MO and the hydrocarbon chains of ILs on the surface of the nano-adsorbent can provide adsorption sites for other organic pollutants through π–π and hydrophobic interactions. Thus, this nano-adsorbent may also find potential application in the extraction and analysis of other organic pollutants.

Acknowledgments

The authors gratefully acknowledge the financial support provided by the Natural Science Foundation of Guangxi Province, China (No. 2013jjDA40029), the Key Project of Guangxi Province Health Department, China (Key. 2011) and the Project of Key Laboratory for the Chemistry and Molecular Engineering of Medicinal Resources (Guangxi Normal University), Ministry of Education of China (CMEMR2013-A-03).

Appendix A. Supplementary material

Supplementary data associated with this article can be found in the online version at http://dx.doi.org/10.1016/j.talanta.2013.11.039.

References

[1] S. Wang, W.X. Xie, X. Zhang, X. Zou, Y. Zhang, Chem. Commun. 48 (2012) 5907–5909.
[2] E. Tahmasebi, Y. Yamini, Anal. Chim. Acta 756 (2012) 13–22.
[3] M. Zhang, X.H. Zhang, X.W. He, L.X. Chen, Y.K. Zhang, Nanoscale 4 (2012) 3141–3147.
[4] Z.Y. He, D.H. Liu, R.H. Li, Z.Q. Zhou, P. Wang, Anal. Chim. Acta 747 (2012) 29–35.
[5] H. Parham, F. Khoshnam, Talanta 114 (2013) 90–94.
[6] Q. Liu, J.B. Shi, J.T. Sun, T. Wang, L.X. Zeng, G.B. Jiang, Angew. Chem. Int. Ed. 50 (2011) 5913–5917.
[7] B. Maddah, J. Shamsi, J. Chromatogr. A 1256 (2012) 40–45.
[8] C.Z. Jiang, Y. Sun, X. Yu, Y. Gao, L. Zhang, Y.P. Wang, H.Q. Zhang, D.Q. Song, Talanta 114 (2013) 167–175.
[9] Y. Liu, H.F. Li, J.M. Lin, Talanta 77 (2009) 1037–1042.
[10] Q. Liu, J.B. Shi, M.T. Cheng, G.L. Li, D. Cao, G.B. Jiang, Chem. Commun. 48 (2012) 1874–1876.
[11] W.N. Wang, R.Y. Ma, Q.H. Wu, C. Wang, Z. Wang, J. Chromatogr. A 1293 (2013) 20–27.
[12] C.Y. Shi, J.R. Meng, C.H. Deng, J. Mater. Chem. 22 (2012) 20778–20785.
[13] Y.B. Luo, Q.W. Yu, B.F. Yuan, Y.Q. Feng, Talanta 90 (2012) 123–131.
[14] Y.X. Wang, S.H. Wang, H.Y. Niu, Y.R. Ma, T. Zeng, Y.Q. Cai, Z.F. Meng, J. Chromatogr. A 1283 (2013) 20–26.
[15] Q. Gao, H.B. Zheng, D. Luo, J. Ding, Y.Q. Feng, Anal. Chim. Acta 720 (2012) 57–62.
[16] X.L. Zhang, H.Y. Niu, Y.Y. Pan, Y.L. Shi, Y.Q. Cai, Anal. Chem. 82 (2010) 2363–2371.
[17] X.L. Zhang, H.Y. Niu, Y.Y. Pan, Y.L. Shi, Y.Q. Cai, J. Colloid Interface Sci. 362 (2011) 107–112.
[18] X.L. Zhang, H.Y. Niu, S.X. Zhang, Y.Q. Cai, Anal. Bioanal. Chem. 397 (2010) 791–798.
[19] Q.H. Wu, G.Y. Zhao, C. Feng, C. Wang, Z. Wang, J. Chromatogr. A 1218 (2011) 7936–7942.
[20] D. Pardasani, P.K. Kanaujia, A.K. Purohit, A.R. Shrivastava, D.K. Dubey, Talanta 86 (2011) 248–255.
[21] N.V. Plechkova, K.R. Seddon, Chem. Soc. Rev. 37 (2008) 123–150.
[22] Z.Q. Tan, J.F. Liu, L. Pang, Trends Anal. Chem. 39 (2012) 218–227.
[23] J.F. Liu, J.A. Jonsson, G.B. Jiang, Trends Anal. Chem. 24 (2005) 20–27.
[24] P. Sun, D.W. Armstrong, Anal. Chim. Acta 661 (2010) 1–16.
[25] A. Berthod, M.J. Ruiz-Ańgel, S. Carda-Broch, J. Chromatogr. A 1184 (2008) 6–18.
[26] H. Ebrahimzadeh, Y. Yamini, F. Kamarei, Talanta 79 (2009) 1472–1477.
[27] C.C. Chang, S.D. Huang, Anal. Chim. Acta 662 (2010) 39–43.
[28] H.H. Bai, Q.X. Zhou, G.H. Xie, J.P. Xiao, Talanta 80 (2010) 1638–1642.
[29] Q.X. Zhou, Y.Y. Gao, G.H. Xie, Talanta 85 (2011) 1598–1602.
[30] X. Zhou, P.F. Xie, J. Wang, B.B. Zhang, M.M. Liu, H.L. Liu, X.H. Feng, J. Chromatogr. A 1218 (2011) 3571–3580.
[31] T.T. Ho, C.Y. Chen, Z.G. Li, T.C.C. Yang, M.R. Lee, Anal. Chim. Acta 712 (2012) 72–77.
[32] V. Pino, J.L. Anderson, J.H. Ayala, V. González, A.M. Afonso, J. Chromatogr. A 1182 (2008) 145–152.
[33] Q.L. Zhang, F. Yang, F. Tang, K. Zeng, K.K. Wu, Q.Y. Cai, S.Z. Yao, Analyst 135 (2010) 2426–2433.
[34] H.D. Qiu, A.K. Mallik, M. Takafuji, X. Liu, S.X. Jiang, H. Ihara, Anal. Chim. Acta 738 (2012) 95–101.
[35] H.D. Qiu, A.K. Mallik, M. Takafuji, H. Ihara, Chem. Eur. J. 17 (2011) 7288–7297.
[36] S.F. Xiao, X.M. Lu, Q.H. Lu, Macromolecules 40 (2007) 7944–7950.
[37] Z.Y. Ma, Y.P. Guan, H.Z. Liu, J. Polym. Sci. Polym. Chem. 43 (2005) 3433–3439.
[38] M.G. Kiseleva, L.V. Radchenko, P.N. Nesterenko, J. Chromatogr. A 920 (2001) 79–85.
[39] C.A. Clayton, J.W. Hines, P.D. Elkins, Anal. Chem. 59 (1987) 2506–2514.
[40] L.A. Currie, Anal. Chim. Acta 391 (1999) 105–126.